Title	Suspension performance with one damper and one inerter
Author(s)	Chen, MZ; Hu, Y; Du, B
Citation	The 24th Chinese Control and Decision Conference (CCDC), Taiyuan, China, 23-25 May 2012. In The 24th Chinese Control and Decision Conference (CCDC) Proceedings, 2012, p. 3534-3539, article no. 6244566
Issued Date	2012
URL	http://hdl.handle.net/10722/160288
Rights	Chinese Control and Decision Conference Proceedings. Copyright © I E E E.

Suspension Performance with One Damper and One Inerter

Michael Z. Q. Chen[1,2,3], Yinlong Hu[3], and Baozhu Du[3]

Abstract—In Chen & Smith 2009, a class of realizations in which the number of dampers and inerters is restricted to one in each case, while allowing an arbitrary number of springs (which is the easiest element to realize practically), was considered and it was proven that at most four springs are needed—an explicit construction was given comprising five different circuit arrangements to cover all cases. This paper makes a comparative study of the performances of these five circuit arrangements when applied as mechanical suspension struts in a quarter-car model.

I. INTRODUCTION

In 2008, two articles in *Autosport* unveiled the mysterious 'J-damper' used in the Formula One Grand Prix races and revealed that the inerter solution was first raced by McLaren in San Marino 2005 and is now adopted by its competitors such as Ferrari [9, 14]. The technical term for this device, however, is *inerter* [15]. (See [4] for more details.)

The inerter is a two-terminal mechanical element with the property that the (equal and opposite) force applied at the terminals is proportional to the relative acceleration between them [15]. In the notation of Fig. 1, the inerter obeys the force-velocity law $F = b(\dot{v}_1 - \dot{v}_2)$, where the constant of proportionality b is called the inertance and has the units of kilograms. Such a device can be constructed using a flywheel that is driven by a rack and pinion, and gears (see Fig. 2).

The rest of the paper is organized as follows. We first present some background on passive network synthesis with the results of [7] in Section II. We then introduce an elementary vehicle suspension model, i.e., the quarter-car model, and define three performance measures of interest in Section III. The optimization results in terms of each individual performance measure are presented in Section IV. Section V considers a multi-objective performance measure which combines two of the three measures and presents the optimization results. Conclusions are given in Section VI.
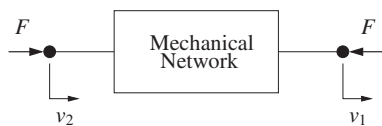

Fig. 1. Free-body diagram of a two-terminal mechanical element with force-velocity pair (F, v) where $v = v_1 - v_2$.

[1]The University of Hong Kong, Department of Mechanical Engineering, Hong Kong. Email: mzqchen@hku.hk. [2]The University of Hong Kong-Shenzhen Institute of Research and Innovation. [3]Nanjing University of Science and Technology, School of Automation, Nanjing, P.R. China.
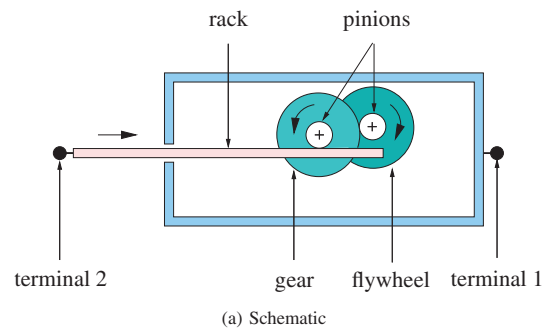
(a) Schematic
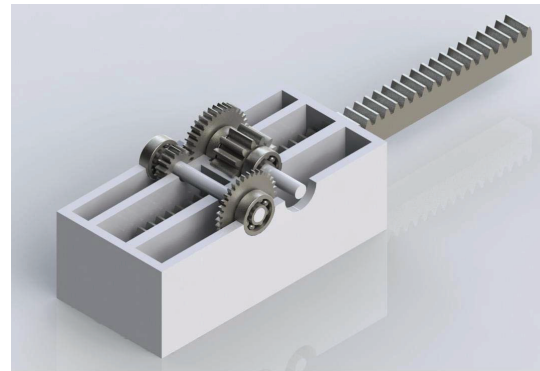
(b) 3D Model

Fig. 2. A rack-pinion inerter.

II. PASSIVE NETWORK SYNTHESIS

One of the principal motivations for the introduction of the inerter in [15] was the synthesis of passive mechanical networks. It was pointed out that the standard form of the electrical-mechanical analogy (where the spring, mass and damper are analogous to the inductor, capacitor and resistor) was restrictive for this purpose, because the mass element effectively has one terminal connected to ground. In order that the full power of electrical circuit synthesis theory be translated over to mechanical networks, it is necessary to replace the mass element by a genuine two-terminal element—the inerter. Fig. 3 shows the new table of element correspondences in the force-current analogy where force and current are the 'through' variables and velocity and voltage are the 'across' variables. The admittance $Y(s)$ is the ratio of through to across quantities, where s is the standard Laplace transform variable. Fig. 4 shows a particular circuit together with a mechanical realization constructed at Cambridge University Engineering Department.

The theory of passive network synthesis has been widely studied [1, 12]. The concept of passivity can be translated over directly to mechanical networks as follows. Suppose that (F, v) represents the force-velocity pair associated with
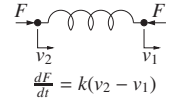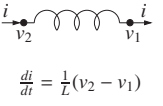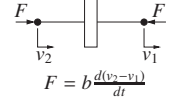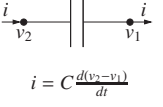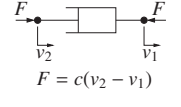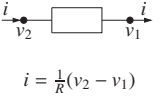
Fig. 3. Circuit symbols and correspondences with defining equations and admittance $Y(s)$.

Fig. 5. General one-port containing one damper and one inerter.

a two-terminal mechanical network, then passivity requires:

$$E(T) = \int_{-\infty}^{T} F(t)v(t)dt \geq 0 \qquad (1)$$

for all admissible force-velocity pairs. If $Z(s)$ is the real rational impedance or admittance function of a linear time-invariant two-terminal network, it is well-known that the network is passive if and only if $Z(s)$ is positive-real [1, 12]. Furthermore, given any positive-real function $Z(s)$, there exists a two-terminal mechanical network whose impedance equals $Z(s)$, which consists of a finite interconnection of springs, dampers and inerters. See [15] for details.

Given the existing and potential applications of the inerter, interest in passive network synthesis has been revived [2, 3, 5–8]. A renewed attempt on the same subject has also been independently advocated by Kalman [10].

In [7], the following problem is solved: what is the most general class of mechanical admittances (or impedances) which can be realized using one damper, one inerter and an arbitrary number of springs and no transformers (levers)? The solution uses element extraction of the damper and inerter (see Fig. 5) followed by the derivation of
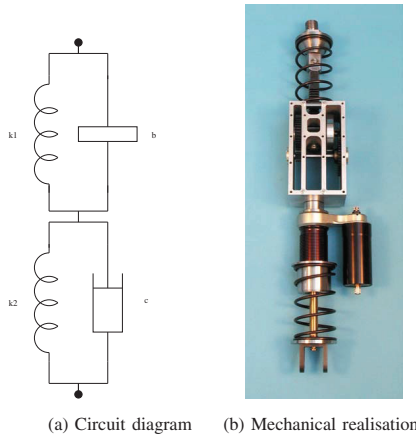

(a) Circuit diagram   (b) Mechanical realisation

Fig. 4. Inerter in series with damper with centring springs constructed at Cambridge University.

a necessary and sufficient condition for the one-element-kind (transformerless) realization of an associated three-port network. In [7], it was proven that at most four springs are needed—an explicit construction was given comprising five different circuit arrangements to cover all cases (see Fig. 6). Other equivalent circuit arrangements can be found in [2, Appendix B].

III. THE QUARTER-CAR MODEL AND PERFORMANCE MEASURES

An elementary model to consider for suspension performance measures is the quarter-car model presented in Fig. 7, which is the simplest model for which meaningful results can be obtained. It consists of the sprung mass m_s, the unsprung mass m_u and a tyre which is modelled as a simple spring with spring stiffness k_t. The suspension strut provides an equal and opposite force on the sprung and unsprung masses and is assumed to be a passive mechanical admittance $Q(s)$ which has negligible mass. The equations of motion in the Laplace transformed domain are:

$$m_s s^2 \hat{z}_s = \hat{F}_s - sQ(s)(\hat{z}_s - \hat{z}_u), \qquad (2)$$
$$m_u s^2 \hat{z}_u = sQ(s)(\hat{z}_s - \hat{z}_u) + k_t(\hat{z}_r - \hat{z}_u). \qquad (3)$$

For comparison, we fix the parameters of the quarter-car model as follows: $m_s = 250$ kg, $m_u = 35$ kg and $k_t = 150$ kN/m, the same as in [17].

We now review the performance measures for vehicle suspensions used in [17]. There are a number of practical design requirements for a suspension system such as passenger comfort, handling, tyre normal loads and limits on suspension travel etc. which require careful optimization. In the quarter-car model these can be translated approximately into specifications on the disturbance responses from F_s and z_r to z_s and z_u. We now define the measures.

We first consider road disturbances z_r. Following [13] a time-varying displacement $z(t)$ is derived from traversing a rigid road profile at velocity V. We let $z(t)$ have the form $z'(x)$ where x is the distance in the direction of motion. Thus $z(t) = z'(Vt)$. The corresponding spectral densities are then
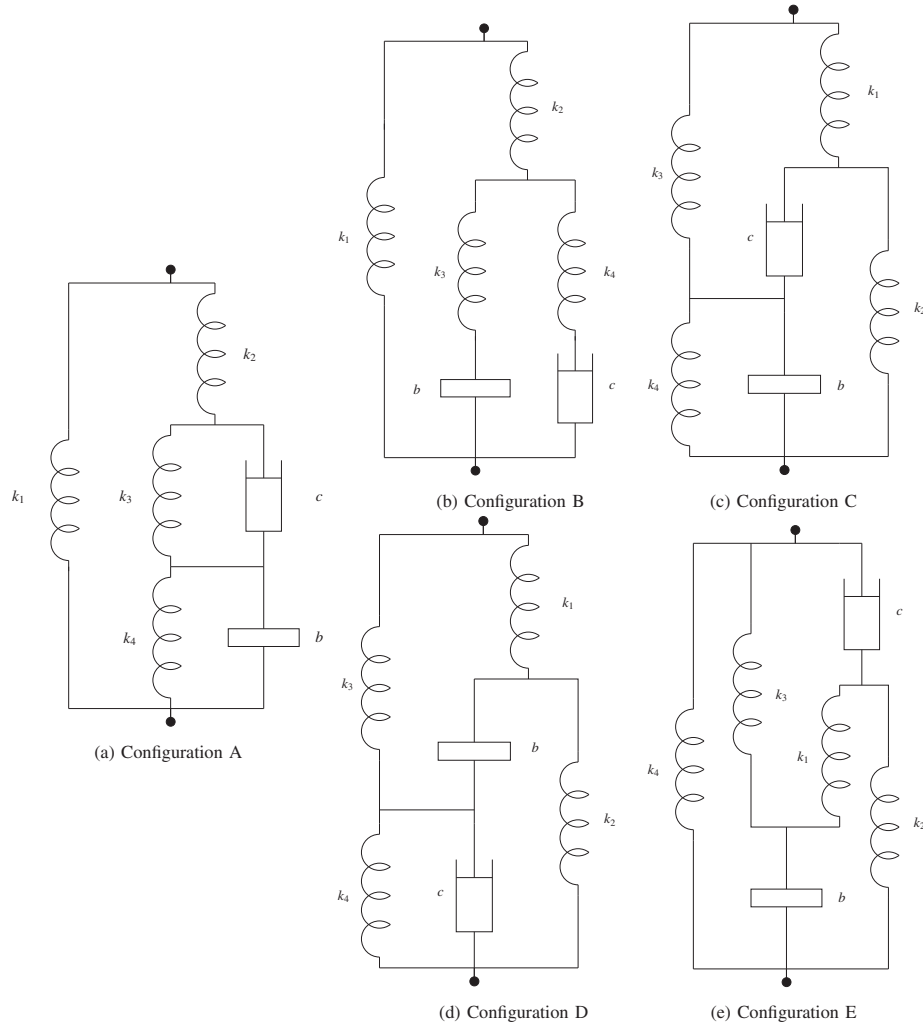
Fig. 6.   Five circuit arrangements considered in [7].

related by

$$S^z(f) = \frac{1}{V} S^{z'}(n)$$

where f is the frequency in cycles/second, n is the wavenumber in cycles/metre and $f = nV$. Now consider an output variable $y(t)$ which is related to $z(t)$ by the transfer function $H(s)$. Then the expectation of $y^2(t)$ is given by:

$$
\begin{aligned}
E\left[y^2(t)\right] &= \int_{-\infty}^{\infty} |H(j2\pi f)|^2 S^z(f) df \\
&= \frac{1}{2\pi} \int_{-\infty}^{\infty} |H(j\omega)|^2 \frac{1}{V} S^{z'}(n(\omega)) d\omega.
\end{aligned}
$$

Here we will use the following spectrum [13]

$$S^{z'}(n) = \kappa |n|^{-2} \qquad \text{(m}^3\text{/cycle)}$$

where κ is a road roughness parameter.

We consider 3 performance measures in this paper, namely J_1, J_3, and J_5. They measure the ride comfort, road holding and dynamic load carrying, respectively. Here, we follow the notation used in [17].

For the ride comfort we use the root-mean-square (r.m.s.) *body vertical acceleration* which is given by

$$
\begin{aligned}
J_1 &= \left(\frac{1}{2\pi V} \int_{-\infty}^{\infty} \left| T_{\hat{z}_r \to \hat{z}_s}(j\omega) \right|^2 \frac{\kappa}{n(\omega)^2} d\omega \right)^{1/2} \\
&= 2\pi \left(V\kappa \right)^{1/2} \| s T_{\hat{z}_r \to \hat{z}_s} \|_2 \qquad (4)
\end{aligned}
$$

where $T_{\hat{z}_r \to \hat{z}_s}$ denotes the transfer function from the road disturbance z_r to the displacement of the sprung mass z_s and $\| \cdot \|_2$ is the standard H_2 norm.

Similarly, to characterize road holding we use the r.m.s. *dynamic tyre load* in response to road disturbance, given by

$$J_3 = 2\pi \left(V\kappa \right)^{1/2} \left\| \frac{k_t}{s} T_{\hat{z}_r \to (\hat{z}_u - \hat{z}_r)} \right\|_2 . \qquad (5)$$

We take $V = 25$ ms^{-1} and $\kappa = 5 \times 10^{-7}$ m^{3}cycle^{-1} (which represents a typical British principal road).

Dynamic load carrying is the ability of the suspension to withstand external loads on the sprung mass, e.g., those induced by braking, accelerating and cornering. Following
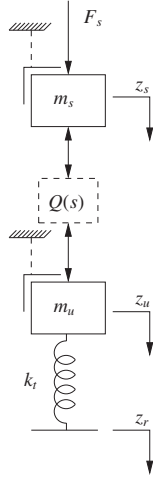
2012 24th Chinese Control and Decision Conference (CCDC)

Fig. 7. Quarter-car vehicle model.

[16], we make use of the following measure for this purpose:

$$J_5 = \left\| T_{\hat{F}_s \to \hat{z}_s} \right\|_\infty \qquad (6)$$

where $\| \cdot \|_\infty$ is the standard H_∞ norm, which is the supremum of the modulus over all frequencies. This norm equals the maximal power transfer function for square integrable signals and hence measures dynamic load carrying.

We rewrite (2) and (3) as

$$\begin{bmatrix} m_s s^2 + sQ(s) & -sQ(s) \\ -sQ(s) & m_u s^2 + k_t + sQ(s) \end{bmatrix} \begin{bmatrix} \hat{z}_s \\ \hat{z}_u \end{bmatrix}$$
$$= \begin{bmatrix} 1 & 0 \\ 0 & k_t \end{bmatrix} \begin{bmatrix} \hat{F}_s \\ \hat{z}_r \end{bmatrix}, \qquad (7)$$

from which we can compute the relevant transfer functions as follows:

$$T_{\hat{z}_r \to \hat{z}_s}$$
$$= \frac{k_t Q(s)}{m_s s(m_u s^2 + k_t) + ((m_u + m_s)s^2 + k_t) Q(s)}, \qquad (8)$$

$$T_{\hat{z}_r \to (\hat{z}_u - \hat{z}_r)}$$
$$= \frac{-s^2 [m_u m_s s + (m_u + m_s)Q(s)]}{m_s s(m_u s^2 + k_t) + ((m_u + m_s)s^2 + k_t) Q(s)}, \qquad (9)$$

$$T_{\hat{F}_s \to \hat{z}_s}$$
$$= \frac{m_u s^2 + k_t + sQ(s)}{s [m_s s(m_u s^2 + k_t) + ((m_u + m_s)s^2 + k_t) Q(s)]}. \quad (10)$$

Substituting (8)–(10) into (4)–(6), we obtain the expressions of J_1, J_3 and J_5, respectively.

IV. OPTIMIZATION OF INDIVIDUAL PERFORMANCE MEASURES

It is a well-known fact [11] that performance measures such as ride comfort, road handling and road holding etc. cannot be optimized (minimized) simultaneously with a passive suspension system. The usual practice of suspension design therefore involves a trade-off between various performance measures. However, it is still useful to consider the individual performances achievable by a particular suspension strut.

It is worth noting that the optimization results of Config. A in Fig. 6 have been presented in [17]. Since Config. A is the best among the circuit arrangements considered within [17], it will serve as the benchmark for our investigation. Optimization results in terms of J_1, J_3 and J_5 are presented in Sections IV-A, IV-B and IV-C, respectively.

The approach is to fix the static stiffness of the suspension strut and then optimize over the remaining parameters. This will be done over a range of static stiffness settings from $k = 10$ kN/m to $k = 120$ kN/m, which covers a range from softly sprung passenger cars through sports cars and heavy goods vehicles up to racing cars. For each of the five suspension struts, the static stiffness is equal to: (A) $k_1 + (k_2^{-1} + k_3^{-1} + k_4^{-1})^{-1}$, (B) k_1, (C) $(k_1^{-1} + k_2^{-1})^{-1} + (k_3^{-1} + k_4^{-1})^{-1}$, (D) $(k_1^{-1} + k_2^{-1})^{-1} + (k_3^{-1} + k_4^{-1})^{-1}$, and (E) $k_4 + (k_1^{-1} + k_2^{-1} + k_3^{-1})^{-1}$.

The Nelder–Mead simplex method was used for various starting points of the optimization and much effort was invested to vary initial parameter values to cover a large range of starting points. Given the relatively small number of parameters, the authors wish to express a cautious opinion that the results represent the global minima.

A. Optimization of J_1 (ride quality)

The optimization results of J_1 are shown in Fig. 8. Config. E is found to be the best among the five. Configs. A and C coincide with Config. E over the higher stiffness range but are outperformed by Config. E over the lower stiffness range. Config. D coincides with Config. E over the lower stiffness range but is outperformed by Config. E over the higher stiffness range. Config. D is better than Config. A over the lower stiffness range but worse over the higher stiffness range. Config. B is the worst performer in terms of performance measure J_1. Therefore, in terms of J_1 we have found one circuit arrangement that outperforms Config. A (Config. E), one circuit arrangement that coincides

Fig. 8. Performance J_1.

with Config. A (Config. C) and one that is a trade-off with Config. A at different stiffness ranges (Config. D).

B. Optimization of J_3 (tyre loads)

The optimization results of J_3 are shown in Fig. 9. Here Config. C is found to be the best among the five. Config. A and Config. E coincide with each other throughout the range. Configs. A and E coincide with Config. C over the higher stiffness range but are outperformed by Config. C over the lower stiffness range. Configs. B and D coincide with Config. C over the lower stiffness range but they diverge and are outperformed by Config. C over the higher stiffness range. Visually, it seems that Config. B is the worst performer in terms of J_3. Therefore, in terms of J_3 we have found one circuit arrangement that outperforms C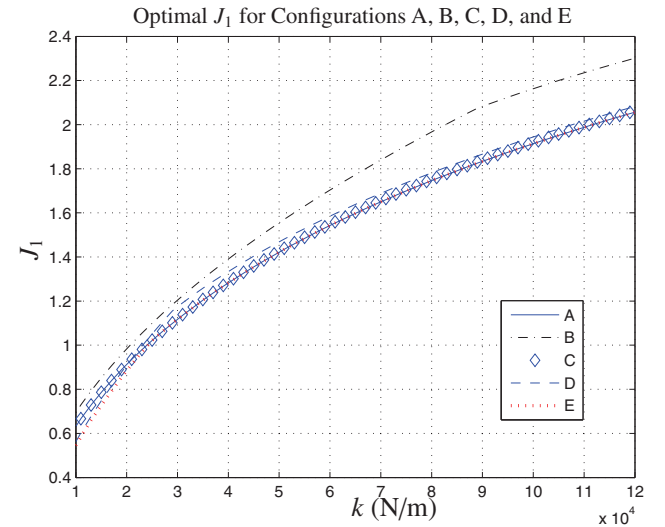onfig. A (Config. C), one circuit arrangement that coincides with Config. A (Config. E) and two that are a trade-off with Config. A at different stiffness ranges (Configs. B and D).

C. Optimization of J_5 (dynamic load carrying)

The optimization results of J_5 over the static stiffness range of 10–240 kN/m are shown in Fig. 10. Here it was found that Configs. B, C, D and E outperform Config. A over the higher stiffness range. There is a theoretical minimum for J_5 equal to the d.c. gain of the transfer function $T_{\hat{F}_s \to \hat{z}_s}$, which is equal to $(k_0^{-1} + k_t^{-1})$ where k_0 is the static stiffness of the suspension. For the static stiffness range of 10–120 kN/m, the J_5 performances of Configs. B, C, D and E manage to coincide with the theoretical minimum of $(k_0^{-1} + k_t^{-1})$ while Config. A diverges at 80 kN/m. Configs. B, C, D and E diverge from the theoretical minimum beyond 120 kN/m and therefore they all manage to beat Config. A in terms of J_5.

It has been observed in [17] that a parallel connection of a damper and an inerter does better than a series connection in terms of J_5. It can be observed that Config. A is essentially a series connection of a damper and an inerter while Config. B is effectively a parallel connection. Configs. C, D and E can be turned into a parallel connection of a damper and an inerter by removing appropriate springs. Therefore, it is expected that the benchmark, Config. A, is outperformed in this category.

V. MULTI-OBJECTIVE OPTIMIZATION

In suspension design, it is usually necessary to consider several performance objectives and thus interesting to investigate whether the five configurations satisfy more than one objective simultaneously. Here we consider J_1 and J_5.

Our approach is to employ a combined performance index:

$$J := \alpha J_1/J_{1,0} + (1 - \alpha)J_5/J_{5,0},$$

for $0 \leq \alpha \leq 1$, with $J_{1,0} = 1.76$ and $J_{5,0} = 2.3333 \times 10^{-5}$ which are the optimal values for a suspension which is a parallel connection of one spring and one damper with static stiffness of $k = 60$ kN/m and optimized over the damper setting c (see [17]). The parallel connection of one spring and one damper is denoted by Config. S.
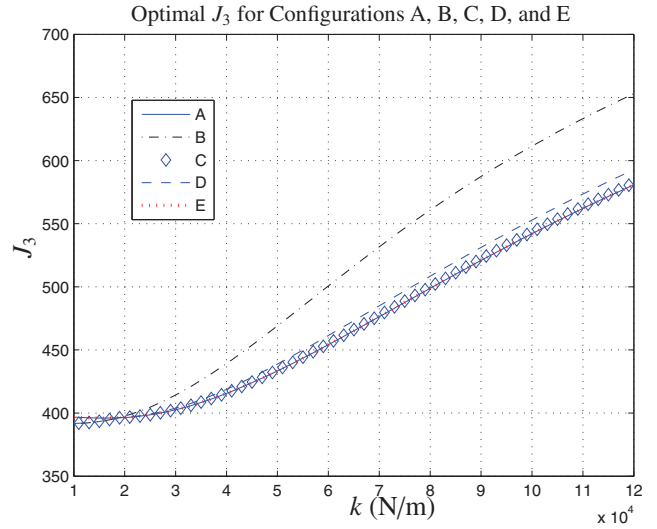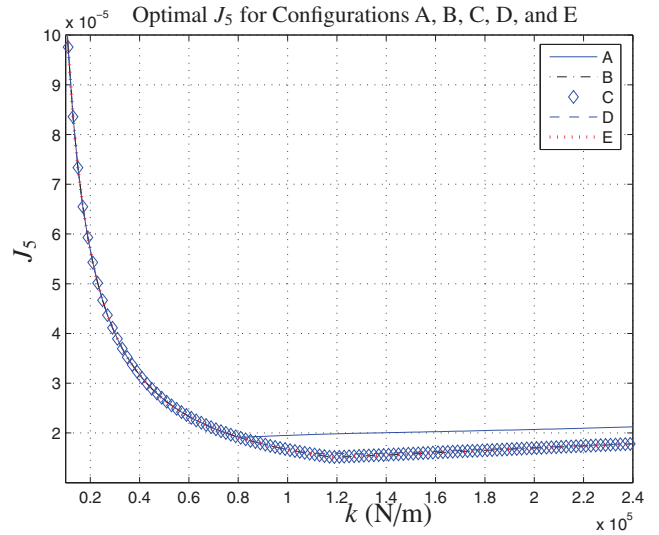

Fig. 9.   Performance J_3.

Fig. 10.   Performance J_5.

The optimization results of the performance index J with respect to α for a static stiffness of $k = 60$ kN/m are shown in Fig. 11. For the range of $\alpha \in [0, 0.86]$, it is clear that Configs. B and E are the best. For the range of $\alpha \in [0.86, 0.91]$, Config. E is the best choice. For the range of $\alpha \in [0.91, 0.95]$, Config. A is the best choice. For the remaining interval of $\alpha \in [0.95, 1]$, Configs. A, C and E coincide and outperform Configs. B and D. Therefore, one circuit arrangement (Config. E) is found to outperform Config. A in terms of the multi-objective performance measure J.

Note that for each configuration the optimization appears to be Pareto optimal, i.e., it is not possible to improve them together in a given configuration (see Fig. 12). Secondly, Config. E is the best from this J_1-J_5 space diagram.

In this paper, we only consider the combination of J_1 and J_5. However, the multi-objective performance index is not necessarily constructed in the same pattern as our J here.
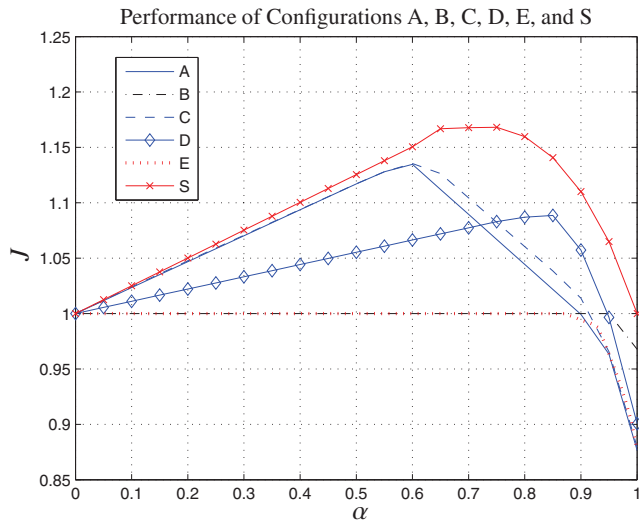
Fig. 11.   Multi-objective performance J vs α.

VI. CONCLUSIONS

The quarter-car model has been reviewed and three performance measures (J_1, J_3 and J_5) were defined. We first investigated each individual performance measure for the five circuit arrangements proposed in [7]. One of the five circuits (Config. A in Fig. 6) has appeared in the literature [17] and therefore serves as the benchmark. We managed to find one or more circuit arrangements that outperform the benchmark for each individual performance measure. Then we investigated a multi-objective performance measure incorporating J_1 and J_5 and found one circuit arrangement (Config. E in Fig. 6) that outperformed the benchmark.

Config. E appears to be the best when all individual and multi-objective performances are considered. This fact might be attributed to the inherent flexibility embedded in Config. E. By setting suitable spring stiffnesses to zero or infinity, Config. E can red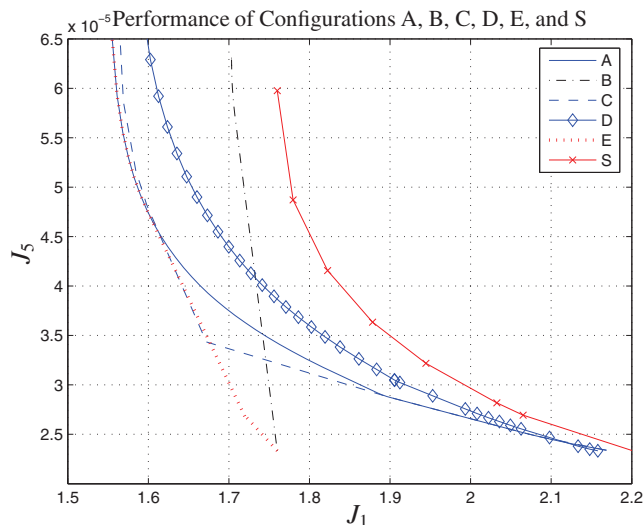uce to a parallel or series connection of the damper and inerter, which possibly provides the flexibility of approaching either if one is favoured when considering a particular performance measure.

We only considered five circuit arrangements. However, each circuit arrangement represents a class of admittances—any circuit capable of realizing the same class, such as those listed in [2, Appendix B], should perform equally.

Although we have investigated different performances of the five proposed circuit arrangements, we have not considered the construction of them in practice. It is expected that Configs. A and B will be easier to implement as they are simple parallel and series constructions while the other three are expected to be more challenging to manufacture as they have Y-connections present. Furthermore, one of the configurations considered in [17] has the potential disadvantage of possible drift of the damper and/or inerter to the limit of travel in the course of operation. The circuit arrangements summarized in Fig. 6 do not appear to have this problem.

REFERENCES

[1] B.D.O. Anderson and S. Vongpanitlerd. *Network Analysis and Synthesis: A Modern Systems Theory Approach*. Prentice-Hall, 1973.
[2] M.Z.Q. Chen. *Passive Network Synthesis of Restricted Complexity*. PhD thesis, University of Cambridge, Cambridge, UK, August 2007.
[3] M.Z.Q. Chen. A note on PIN polynomials and PRIN rational functions. *IEEE Trans. on Circuits and Systems II-Express Briefs*, 55(5):462–463, 2008.
[4] M.Z.Q. Chen, C. Papageorgiou, F. Scheibe, F.-C. Wang, and M.C. Smith. The missing mechanical circuit element. *IEEE Circuits and Systems Magazine*, 9(1):10–26, 2009.
[5] M.Z.Q. Chen and M.C. Smith. *Recent Advances in Learning and Control*, chapter III, pages 35–50. Springer, 2008.
[6] M.Z.Q. Chen and M.C. Smith. A note on tests for positive-real functions. *IEEE Trans. on Automatic Control*, 54(2):390–393, 2009.
[7] M.Z.Q. Chen and M.C. Smith. Restricted complexity network realizations for passive mechanical control. *IEEE Trans. on Automatic Control*, 54(10):2290–2301, 2009.
[8] M. Hakimi-Moghadam and H. Khaloozadeh. Strict positive realness and its equivalent electrical networks. In *2011 Chinese Control and Decision Conference (CCDC)*, 2011.
[9] M. Hughes. A genius idea, and why McLaren hasn't tried to stop others using it. *Autosport*, 29 May 2008.
[10] R. Kalman. *Perspectives in Mathematical System Theory, Control, and Signal Processing*, chapter I, pages 3–13. Springer, 2010.
[11] D. Karnopp. Theoretical limitations in active suspensions. *Vehicle System Dynamics*, 15:41–54, 1986.
[12] R.W. Newcomb. *Linear Multiport Synthesis*. McGraw-Hill, 1966.
[13] J.D. Robson. Road surface description and vehicle response. *Int. J. of Vehicle Design*, 1(1):25–35, 1979.
[14] C. Scarborough. Technical insight: Renault's J-damper. *Autosport*, 7 May 2008.
[15] M.C. Smith. Synthesis of mechanical networks : the inerter. *IEEE Transactions on Automatic Control*, 47(10):1648–1662, 2002.
[16] M.C. Smith and G.W. Walker. A mechanical network approach to performance capabilities of passive suspensions. In *Workshop Modelling and Control of Mechanical Systems*, London, UK, June 17-20 1997. Imperial College.
[17] M.C. Smith and F-C. Wang. Performance benefits in passive vehicle suspensions employing inerters. *Vehicle System Dynamics*, 42, 2004.

Fig. 12.   Multi-objective performance J_5 vs J_1.